Continental Shelf Research 32 (2012) 47–61

Contents lists available at SciVerse ScienceDirect

Continental Shelf Research

journal homepage: www.elsevier.com/locate/csr

Research papers

The influence of large-scale circulation, transient and local processes on the seasonal circulation of the Eastern Brazilian Shelf, 13°S

F.N. Amorim [a,b,*], M. Cirano [b,d], I.D. Soares [c], E.J.D. Campos [a], J.F. Middleton [d,e]

[a] Instituto Oceanográfico da Universidade de São Paulo, São Paulo, Brazil
[b] Grupo de Oceanografia Tropical, Instituto de Física, Universidade Federal da Bahia, Salvador, Brazil
[c] Associação Atlantis, Brazil
[d] Aquatic Sciences, South Australia Research and Development Institute, Adelaide, Australia
[e] School of Mathematical Sciences, University of Adelaide, Adelaide, Australia

ARTICLE INFO

Article history:
Received 26 May 2011
Received in revised form
22 September 2011
Accepted 19 October 2011
Available online 4 November 2011

Keywords:
Shelf currents
Wind-driven circulation
Western Boundary Currents
South Equatorial Current
Salvador Canyon
Cold Front systems

ABSTRACT

The circulation at the Eastern Brazilian Shelf (EBS), near 13°S, is discussed in terms of the currents and hydrography, associating large-scale circulation, transient and local processes to establish a regional picture of the EBS circulation. The results show that the circulation within the continental shelf and slope region is strongly affected by the seasonal changes in the wind field and meso/large-scale circulation. Transient processes associated to the passage of Cold Front systems or meso-scale activity and the presence of a local canyon add more complexity to the system. During the austral spring and summer seasons, the prevailing upwelling favorable winds blowing from E–NE were responsible for driving southwestward shelf currents. The interaction with the Western Boundary Current (the Brazil Current), especially during summer, was significant and a considerable vertical shear in the velocity field was observed at the outer shelf. The passage of a Cold Front system during the springtime caused a complete reversal of the mean flow and contributed to the deepening of the Mixed Layer Depth (MLD). In addition, the presence of Salvador Canyon, subject to an upwelling favorable boundary current, enhanced the upwelling system, when compared to the upwelling observed at the adjacent shelf. During the austral autumn and winter seasons the prevailing downwelling favorable winds blowing from the SE acted to total reverse the shelf circulation, resulting in a northeastward flow. The passage of a strong Cold Front, during the autumn season, contributed not only to the strengthening of the flow but also to the deepening of the MLD. The presence of the Salvador Canyon, when subject to a downwelling favorable boundary current, caused an intensification of the downwelling process. Interestingly, the alongshore velocity at the shelf region adjacent to the head of the canyon was less affected when compared to the upwelling situation.

1. Introduction

The continental shelf along the state of Bahia, NE Brazil, encompasses almost the entire extension of the Eastern Brazilian Shelf (hereinafter EBS). The EBS is geographically limited between 13°S and 22°S (Knoppers et al., 1999) and apart from the Abrolhos Bank, on its southernmost position, it represents the narrowest straight continental shelf along the Brazilian coastline (average width of 17 km at the study region). In the world context, this turns the EBS into a peculiar region, since narrow shelves are not a common feature along passive continental margins.

The oceanography of the EBS is highly influenced by the northern limb of the subtropical gyre, where the bifurcation of the South Equatorial Current (SEC), at its upper level, originates the two major shelf/slope Western Boundary Currents (WBC): the poleward Brazil Current (BC) and the equatorward North Brazil Current/North Brazil Undercurrent (NBC/NBUC). While in some regions, mesoscale processes related to the WBCs influence only the outer shelf region, as observed at the South Atlantic Bight (e.g. Allen et al., 1983; Lee et al., 1984), here, as reported by Amorim et al. (2011), these features can also influence the mid-shelf region, causing events of complete reversals of the shelf currents.

The meteorological forcings at the EBS and adjacent offshore region are subject to a strong meridional wind seasonal cycle associated to the variability in the amplitude of the local wind stress curl, due to the annual north–south displacement of the marine Inter-tropical Convergence Zone—ITCZ (Dominguez, 2006; Rodrigues et al., 2007). As an ocean response, the SEC bifurcation also undergoes a seasonal latitudinal excursion (Fig. 1). According to Rodrigues et al. (2007), during the austral spring/summer, local positive wind stress curl produces an anomalous anti-cyclonic

* Correspondence to: Cidade Universitária, Praça do Oceanográfico, 191, 05508-900, São Paulo, Brazil.
E-mail addresses: fnamorim@gmail.com, fnamorim@usp.br (F.N. Amorim).

0278-4343/$ - see front matter © 2011 Elsevier Ltd. All rights reserved.
doi:10.1016/j.csr.2011.10.011

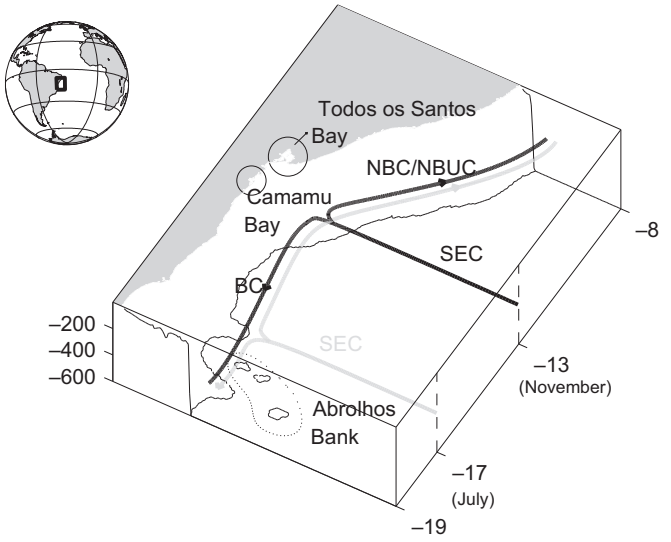

Fig. 1. Schematic seasonal variation of the Western Boundary Currents (WBC) at the upper levels along the East Brazilian Shelf/slope region. The gray line shows the southernmost (17°S in July) position of the bifurcation of the South Equatorial Current (SEC), while the black line shows the northernmost position (13°S in November) of the bifurcation of the SEC according to Rodrigues et al. (2007). The poleward WBC is the Brazil Current (BC) while the equatorward WBC is the North Brazil Current/North Brazil Undercurrent System (NBC/NBUC). The locations of the important ecosystems are also shown.

circulation which moves the SEC bifurcation northward. Conversely, local negative wind stress curl during the austral winter produces an anomalous cyclonic circulation, causing a southward shift of the SEC bifurcation. According to these authors, this latitudinal excursion is strongest in the top 400 m, reaching its southernmost (northernmost) position ~17°S in July (~13°S in November).

In a more recent study, Soutelino et al. (2011) showed that the near surface (50 m) flow at the shelf/slope region of the SEC bifurcation is associated with eddy structures. These authors argue that between 15°S and 20°S, the BC could be interpreted as the flow composed by the coastal border of three robust anticyclones. North of this latitude, a cyclonic structure might be associated with the start of the surface NBC.

The remote wind forcing is also an important driving mechanism in the local hydrodynamics. Following the large scale seasonality of the trade wind regime, the EBS circulation is mainly driven by winds from E/SE to the north of 20°S during the autumn/winter seasons, and by winds from NE to the south of 12°S during the spring/summer seasons (Dominguez, 2006), presenting very distinct scenarios between seasons, with a complete reversal of the mean shelf flow (Amorim et al., 2011). These authors also point to the importance of the passage of atmospheric Cold Front systems along the EBS, which according to the season, are related to episodic reversals of the preferential shelf flow.

In addition to the complexity of the EBS system forcing mechanisms presented above, the topography of the EBS is also marked by the presence of few submarine canyons. According to Allen and Durrieu de Madron (2009), these topographic features are conduits of enhanced transport between the shelf and the deep ocean and could strongly affect the local circulation. The literature on the dynamics of narrow canyons has fortunately increased during the last few decades. For the Astoria Canyon, at the northwestern coast of North America, She and Klinck (2000) based on numerical modeling have shown that for upwelling favorable winds, the onshore cross-shore pressure gradient that supports the alongshore geostrophic flow, when interacting with the canyon topography, breaks the geostrophic constraint and drives water into the canyon, inducing upwelling. This upwelled water is larger than the wind-driven upwelling along the adjacent shelf break and is capable of rising water from depths up to 300 m below the canyon rim. Kampf (2006) also suggests that for an upwelling wind system, the up-canyon flow is a response of the rapid geostrophic adjustment to barotropic pressure gradients established across the canyon and the disturbances in the density field operate to enhance the canyon upwelling process, with the formation of a cyclonic eddy within the canyon as a major effect of the stratification. For downwelling favorable winds, the opposite situation occurs and an anticyclone is formed (She and Klinck, 2000). These authors point out that the circulation near the top of the canyon, in this situation, is more alongshore oriented, while for upwelling favorable winds it is mainly cross-shore oriented.

As it had been shown, the EBS is a very interesting region in terms of hydrodynamics. Due to its narrow shelf, the WBC originated from the SEC bifurcation and the mesoscale processes associated with these WBCs are expected to interact closely with the wind-driven shelf currents. All of these processes have indeed a significant seasonal cycle. But, although these forcings mechanisms were to some extent addressed isolatedly in few selected works, until now, no attempt has been made to combine them to elucidate the dynamics of the seasonal circulation of the EBS. With this purpose, and focusing on the central coast of Bahia (around 13°S), this study aims to establish a first regional picture on the influence of large-scale circulation and transient processes, as well as local topographic features, on the seasonal EBS circulation.

To accomplish this task, a set of original *in situ* oceanographic data (hydrography and currents) sampled along the shelf and slope region, covering the four austral seasons, is explored. The paper is organized as follows. The regional setting of the study area is presented in Section 2. Data and the methodologies adopted are given in Section 3. Section 4 describes the major results relating the wind pattern during the cruise days with the hydrodynamics and thermohaline structure. Finally, an integrated discussion of the results is presented in Section 5.

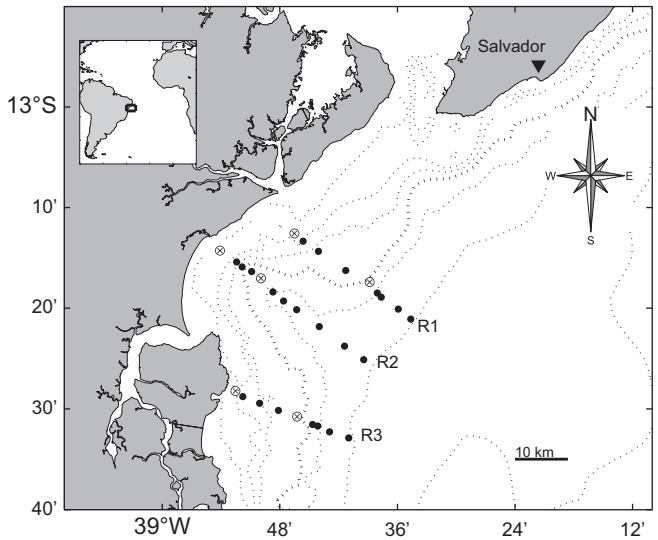

Fig. 2. Location map of the study region. R1, R2 and R3 are the transects, where the • symbols represent the CTD stations (1–9 at R1 and R3 and 1–11 at R2) and the ⊗ symbols delimit the ADCP transects. The isobaths are represented by the 10 m, 20 m, 30 m, 50 m, 200 m, 1000 m and 2000 m contours. The 50 m isobath, which represents the shelf-break and the Salvador canyon rim, is in bold. The Salvador Canyon is located at transect R2.

2. Regional setting

The region of study is located at the central coast of the state of Bahia, in NE Brazil (13°S; Fig. 2), just south of the place where the EBS reaches its narrowest width (~7 km). The shelf break is situated at about 50–60 m.

As mentioned in Section 1, due to the narrowness of the shelf, the adjacent WBC and its associated mesoscale activity is expected to influence the shelf dynamics. Since the latitude of the SEC bifurcation, at the upper levels, changes seasonally, a possible change in the direction of the WBC is also expected to occur during the annual cycle. Due to: (i) the lack of available data and (ii) the fact that there are several ways of defining a WBC, the origin of both the northward NBC and the southward BC is somehow difficult to define (see Fig. 4 of Stramma and Schott, 1999). Here, we adopt the change in the direction of the annual mean velocity at several cross-sections obtained from 13 years of drifting buoys from Oliveira et al. (2009) to position the origin of the NBC and BC at 10°S and 15°S, respectively. The regional circulation associated to the WBCs during the cruise periods is discussed in more detail in Section 4.2.

While the NBC is an intense equatorward WBC (Silveira et al., 1994), at its origin, the poleward BC is a weak and shallow (~100 m) flow, generally associated with the warm and salty Tropical Water ($T > 20^{\circ}$ C, $S > 36$ and $\sigma_{\theta} < 25.7$ kg m^{-3}). As the BC flow southwards, it not only is strengthened but also deepens, eventually incorporating the upper thermocline water of the South Atlantic Central Water. According to the literature though, that only occurs near 22°S (Stramma and England, 1999; Silveira et al., 2000; Cirano et al., 2006). Due to that, at the region of study, the upper thermocline water, underneath the surface layer, always flows northward carried by the NBUC. This permanent northward flow at the NBUC level is clearly shown at 14°S, on the numerical modeling results from Rezende et al. (2011).

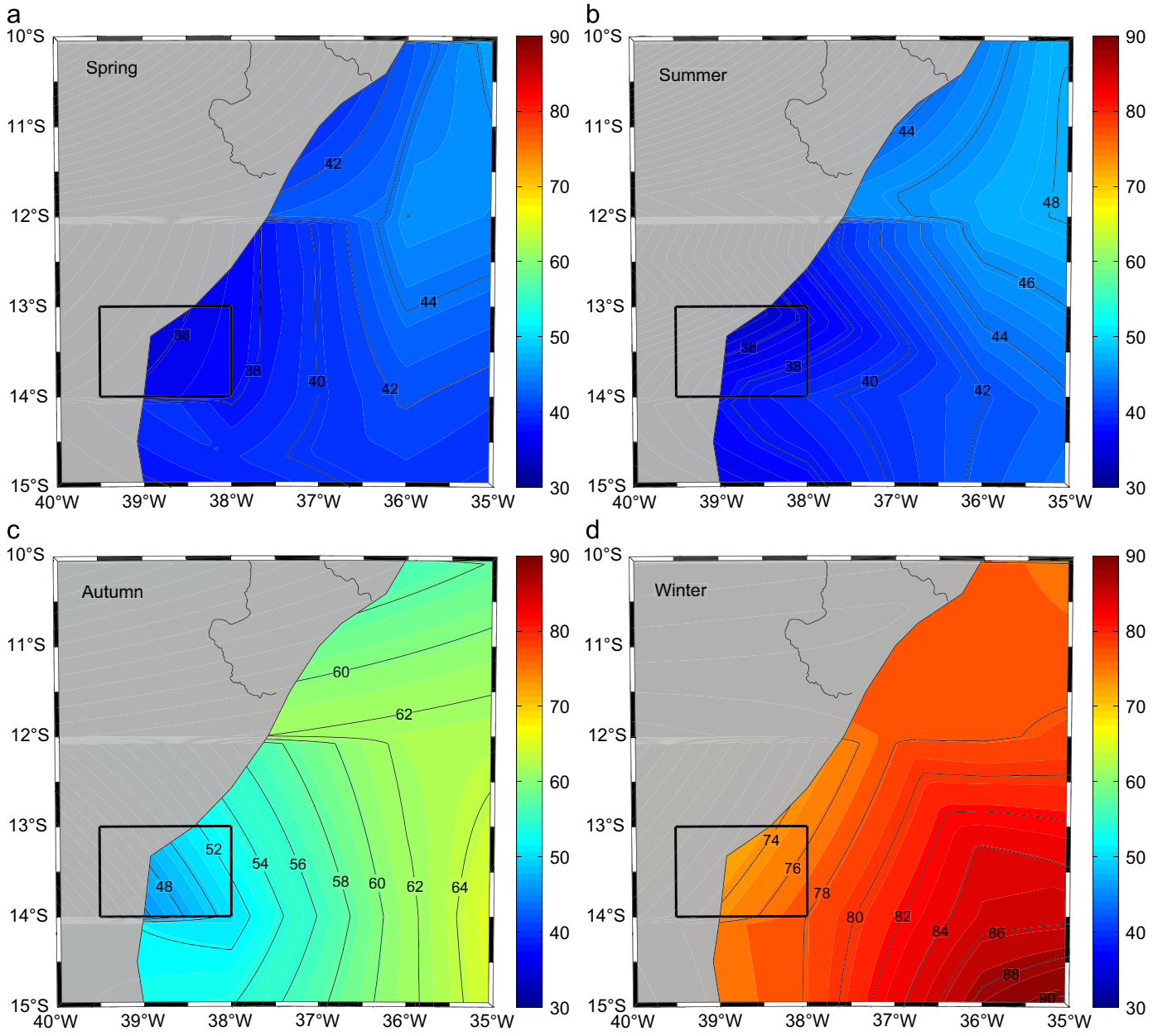

Fig. 3. The seasonal Mixed Layer Depth (MLD) over the study area derived from the global MLD climatology proposed by Montégut et al. (2004) for (a) spring, (b) summer, (c) autumn and (d) winter. The box indicates the region of study.

The upper surface water is strongly affected by the local winds and surface air temperature changes, which contribute to a remarkable change in the mixed layer depth (MLD) between seasons. The MLD here is based on the temperature criteria defined by Montégut et al. (2004) that uses a 0.2°C threshold value calculated from the temperature at 10 m depth. According to these authors, the use of this depth avoids a large part of the strong diurnal cycle in the top few meters of the ocean. Since the Montégut et al. (2004) MLD climatology has a $1^\circ \times 1^\circ$ horizontal resolution, we have to take into account that it does not have enough resolution to include the effect of abrupt changes in topography on the local MLD, reflecting mostly the shelf-wide pattern. For the region of study, the Montégut et al. (2004) seasonal climatology of the MLD (Fig. 3) shows values varying from about 35 m in summer to 75 m in winter. A springtime re-stratification is also well defined with values close to those observed during the summertime.

In terms of the seasonality of the shelf currents, the only reference available in the literature is related to Amorim et al. (2011). Their results are based on two current-meter shelf moorings covering the 2002/2003 austral summer and the 2003 austral autumn and, as pointed out in Section 1, show that the currents at the shelf are mainly wind driven, experiencing a complete reversal between seasons due to a similar change in the wind field. Their results also show that at the inner-shelf (local depth of 28 m), the alongshore velocity was mostly driven by forcings at the sub-inertial frequency. While at the mid-shelf (local depth of 42 m), a similar pattern was also observed, a larger contribution of the sub-inertial forcings was found during autumn. The authors argued that this could be related to a weaker autumn stratification, resulting in a more barotropic signature.

The influence of tides in the region is of secondary importance. Amorim et al. (2011), for the data described above, have shown that the near surface tidal currents account for up to 31% and 22% of the variability of the cross-shore and alongshore components of the velocity, respectively. In addition Pereira et al. (2005), studying the tide–topography interaction along the EBS from 14°S to 19°S, found that the northern portion of their region (vertical slice f in their Fig. 1), which is the closest location to our study region, is the least affected by internal tides.

As mentioned in Section 1, the presence of abrupt changes in topography could add more complexity to the circulation and associated thermohaline field. Fig. 2 shows the location of Salvador Canyon, which is a quite long ($\sim$24 km) and narrow canyon with an axial bottom depth (H) of 450 m and a half-width (L) of 7.7 km, giving an aspect ratio (H/L) of 0.06. The canyon is relatively symmetrical in shape and roughly aligned perpendicular to the local isobaths, that is to say that the geostrophic alongshore currents, which follow the NE–SW direction of the local isobaths, intersect the canyon axis at right angles. To evaluate the influence of the canyon topography in the local circulation, and following Hickey (1997), the stratification parameter ($S = NH/fL$) and relevant length scales such as the vertical stratification scale ($T_r = fL/N$) and the internal Rossby radius of deformation ($R_d = NH/f$) are provided. Each of these parameters depend on the latitude, through the Coriolis parameter (f), and on the stratification, through the buoyancy frequency (N^2). For the study region $f = -3.4 \times 10^{-5}\ s^{-1}$ and based on the in situ data that are presented in Section 4, the buoyancy frequency varies from $5.5 \times 10^{-3} < N < 6.9 \times 10^{-3}\ s^{-1}$, the stratification parameter range is $9 < S < 12$, the vertical stratification scale range is about $50 < T_r < 40$ m and the internal Rossby radius range is about $70 < R_D < 90$ km for weak (winter) and strong (summer) stratification, respectively. As a consequence, the Salvador Canyon will certainly affect the circulation and a dynamics similar to what was described in Section 1 is expected to occur.

3. Data and methods

Hydrographic surveys, covering of the four austral seasons, were carried out during the following periods: (i) 17–24 October 2006—austral spring, (ii) 24–28 January 2007—austral summer, (iii) 9–16 May 2007—austral autumn and (iv) 2–5 August 2007—austral winter. In each survey, temperature and salinity casts were sampled along 29 hydrographic stations distributed in three cross-shelf transects (Fig. 2). Additionally, velocity profiles for the shelf region were also registered along each transect using a bottom-tracking ADCP. In order to minimize possible secondary effects of tides, as reported in Hickey (1997) for the Astoria Canyon, all the samplings at the R2 transects were performed during the neap tide, with ADCP profiling preferably being performed close to the slack water, which was the case for the spring and summer cruises.

The hydrographic measurements were taken with a *SBE 19 plus SEACAT Profiler Seabird* CTD, with a sampling frequency of 4 Hz. The vertical profilers reached a maximum depth of 500 m, due to the instrument limitations. The current measurements were made with a *Workhorse 600 kHz RD* ADCP, registering the currents structure between the 10 m and 50 m isobaths (Fig. 2), due to the instrument range. However, for the transect R2, the deeper limit of the ADCP transect was placed between the 50 m and 200 m isobaths in order to have a better representation of the current dynamics at the canyon axis. The equipment was set up with 2 m vertical resolution cells, performing temporal means of four ensembles at a sampling frequency of 4 Hz.

The hydrographic data were subsequently filtered to remove possible spikes and then a bin average was carried out (Emery and Thomson, 1997). Hydrodynamics will be evaluated, among other criteria, based on the MLD evolution, which is capable to capture important features in the global ocean and plays a key role in several ocean processes (Montégut et al., 2004; Gonzalez-Pola et al., 2007). The MLD defines the extent of turbulent penetration into the ocean due to air–sea fluxes, establishing the atmosphere–ocean heat exchange regime (Gonzalez-Pola et al., 2007). The MDL will be evaluated based on the same criteria used for the Montégut et al. (2004) climatology, described in Section 2.

The currents were rotated based on the orientation of each transect relative to the true north (°T), which were 33°T, 37.8°T and 18°T for transects R1, R2 and R3, respectively. Depth-averaged velocity vectors were calculated based on the vertical distribution of these currents. The AVISO Ssalto/Duacs Gridded Absolute Dynamic Topography and absolute geostrophic velocities ($1/3^\circ \times 1/3^\circ$ horizontal resolution) obtained from AVISO (2011) were also used to provide information on the regional and large-scale circulation at the seasonal cruises.

The regional wind field was investigated for the whole month where each cruise took place in order to establish a relationship with regional circulation dynamics. The data were based on a 3-hourly oceanic meteorological station (INPE, 2009b) located at Salvador city, distant approximately 42 km from the region of interest (Fig. 2). Since most of the analyses are made for offshore data (depths > 100 m), we applied a correction on the meteorological station data based on the criterion proposed by Hsu (1986), which relates the wind sea data with the wind land data according to the equation $U_{sea} = 1.62 + 1.17U_{land}$, where U is the wind speed. This criterion is recommended for operational use and climatological applications and strongly agrees with the criterion proposed by Liu et al. (1984), which takes the air–sea temperature differences into consideration (see Fig. 3 from Hsu, 1986). Wind data derived from the NCEP Reanalysis II (Kanamitsu et al., 2002) for a point located in the center of the study region were also taken into consideration and the data showed similar intensity values when compared to the corrected data from the

meteorological station, but due to the low temporal resolution of the first (6-hourly), the NCEP data were discarded.

4. Results and discussion

In order to have a better understanding of the results, which are discussed primarily in terms of the seasons, it is important to mention that at each cruise, the transects were performed within a variable time window of 3–7 days. This also allows us to discuss the effects of transient processes in the local circulation. Considering that the meteorological forcing is an important part of the local dynamics, a brief contextualization on the general patterns of the winds before and after each seasonal cruise is provided in Section 4.1. With this scenario in mind, an overview of the regional meso/large scale circulation derived from AVISO, for each cruise or at the closest date available, is analyzed together with the shelf circulation derived from the ADCP data in Section 4.2. Finally, Section 4.3 presents the hydrographic data, focusing on the general patterns of the temperature and salinity observed during the cruises.

4.1. The wind regime

During the spring cruise, the prevailing winds were from the E–NE with a mean velocity of 2.9 m s^{-1} (Fig. 4a). Between 21–22 October and before the occupancy of transect R1, a Cold Front passage was registered (INPE, 2009a). At that stage, winds reversed from the SE, with the mean velocity polarized at the alongshore direction, with an intensity of 5.7 m s^{-1}, a value almost twice of the monthly mean. For the summer cruise, there were no records of a Cold Front passage and winds followed the preferential direction for this season, blowing from the E–NE with a mean intensity of 3.7 m s^{-1} during the cruise days (Fig. 4b). The alongshore component of the wind was quite weak, with a mean of -1.34 m s^{-1}.

During the autumn campaign the mean wind intensity was 2.6 m s^{-1}, but, a strong Cold Front was registered before the occupancy of transects R1 and R2, and a magnification of the SE winds occurred, reaching a mean intensity of 6.6 m s^{-1} (Fig. 4c). Finally, the winter cruise was made under typical wintertime conditions, with mean SE winds of 3.6 m s^{-1}. However, intensity

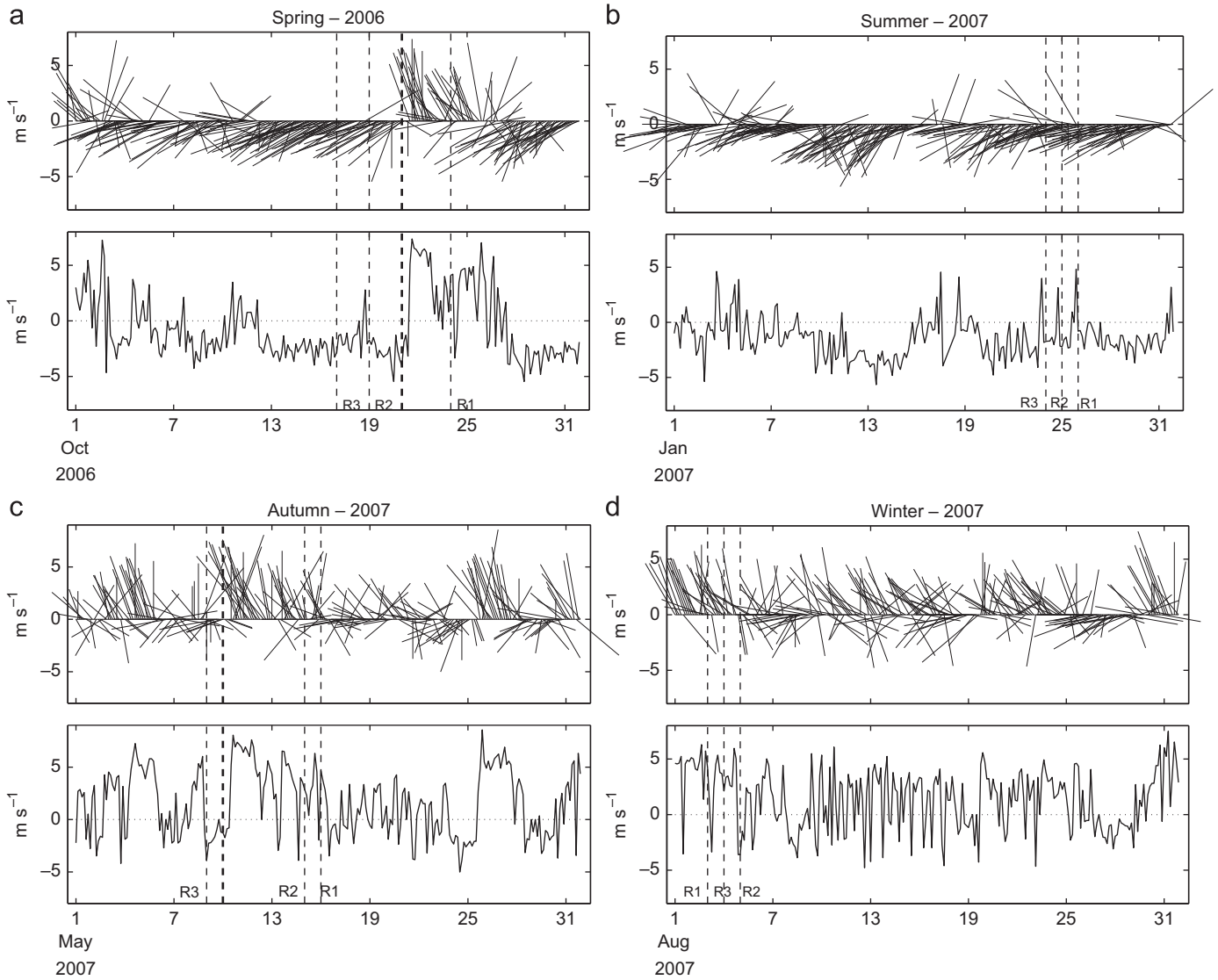

Fig. 4. The wind field observed at the Salvador meteorological station (INPE, 2009b) during the month where the (a) spring, (b) summer, (c) autumn and (d) winter cruises were conducted. At each graph the top panel represents the stick-plot of the wind vectors while the bottom panel represents the alongshore component of the wind. The vertical light-dashed lines mark the days where each transect (R1, R2 and R3) was conducted during the cruise, while the heavy-dashed lines mark the days where a Cold Front passage was registered. The vertical axis in the top panel is North–South oriented.

peaks greater than $+5.0\ m\ s^{-1}$ were registered for the alongshore component of the wind during the cruise days (Fig. 4d).

4.2. The shelf and shelf/slope circulation

Before describing the shelf currents derived from the ADCP at the transects R1–R3 during the seasonal cruises, it is important to provide an overview of the circulation at the shelf/slope region during the cruise periods, so that the influence of the WBC can be evaluated in the area. According to Amorim et al. (2011), the circulation on the inner and mid-shelf is strongly related to the wind pattern, however, meso-scale activity associated to the WBC flowing at the shelf/slope can influence periodically the circulation within the shelf, causing significant current reversals.

For this purpose, maps of the AVISO surface geostrophic currents and associated dynamic topography (AVISO, 2011)

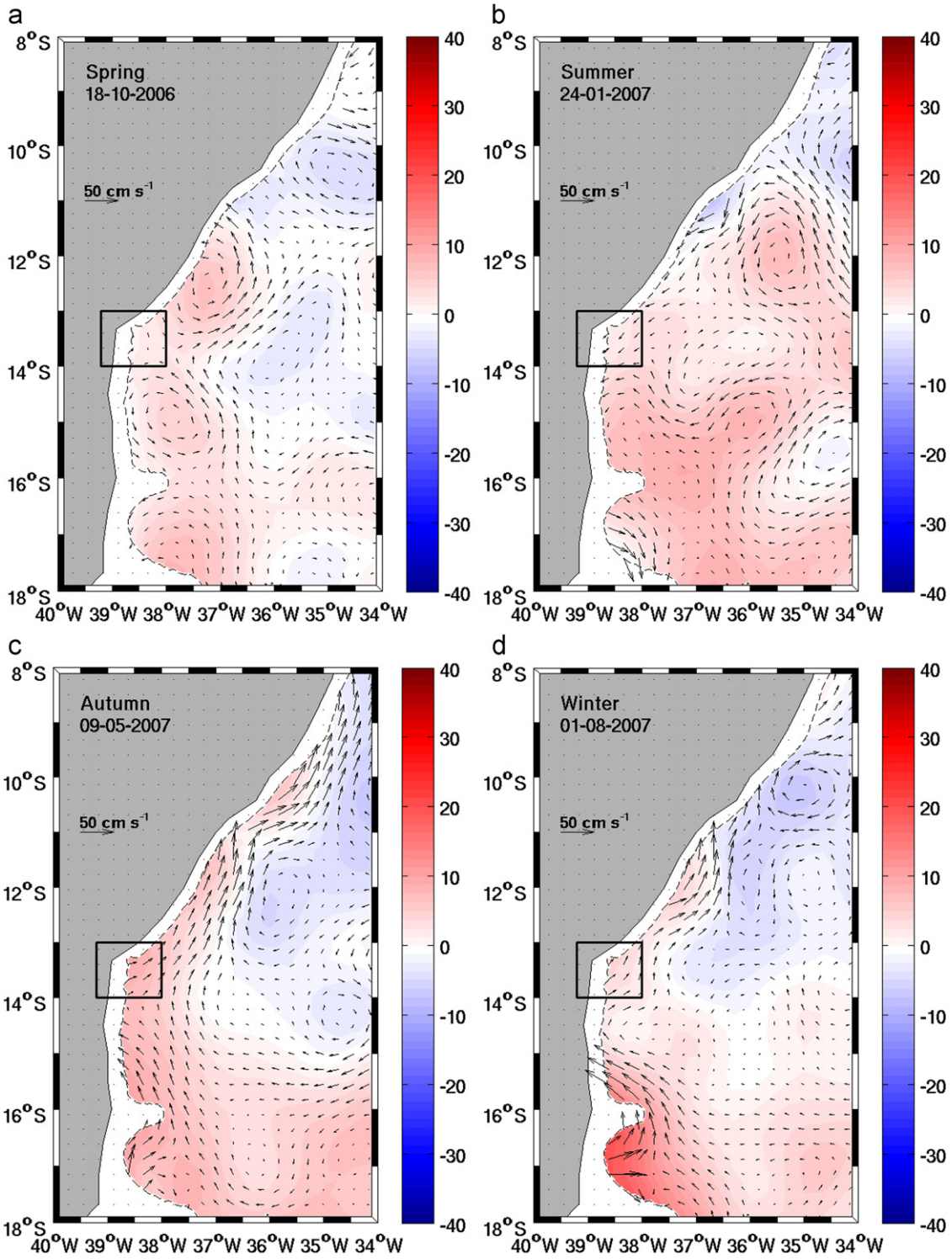

Fig. 5. Maps of geostrophic velocity and absolute dynamic topography (in shading color) derived from AVISO for the closest available day of the (a) spring, (b) summer, (c) autumn and (d) winter cruises. The mean topography was subtracted from the plots to facilitate inter-comparison. Data are only presented at depths greater than 200 m. The box indicates the region of study. (For interpretation of the references to color in this figure legend, the reader is referred to the web version of this article.)

for the shelf/slope (depths >200 m) were obtained for the closest available day at each seasonal cruise and are presented in Fig. 5.

The shelf/slope circulation during the spring cruise (Fig. 5a) shows three anti-cyclones occupying the region from 12°S to 18°S, leading to a southward current at this region, a similar pattern of the BC north of 20°S described by Soutelino et al. (2011). At the oceanic portion of the region, one can also clearly notice the westward oriented flow of the SEC, which is associated with these anti-cyclones. The scenario at the summer cruise (Fig. 5b) is somehow similar to was observed during the spring cruise, with the exception that the shelf/slope region is less dominated by eddies and that the westward SEC is now a broader flow.

During the autumn cruise (Fig. 5c), the circulation at the shelf/slope region and north of 15°S is now defined as a continuous N/NE oriented flow, mostly driven by the bifurcation of the westward SEC flow that enters the region south of 15°S. The offshore sea surface gradient that supports this flow is evident along the whole region. During the winter cruise (Fig. 5d), the general pattern of the shelf/slope flow is somehow similar, but now the meso-scale features are more evident, such as the large cyclonic feature that occupies the region from 10°S to 14°S.

With the circulation at the shelf/slope region in mind, one can now analyze the shelf circulation (between the 10 m and 50 m isobaths) based on the horizontal distribution of the depth-averaged currents derived from the three ADCP transects obtained during the seasonal cruises (Fig. 6) and some vertical sections of the horizontal velocity components at these transects to illustrate specific details (Figs. 7–10).

During the spring and summer season the prevailing upwelling favorable E–NE winds (Fig. 4a and b) acted to drive the southward shelf currents at transect R3 (Fig. 6a and b). At transect R2, although the measurements were still under typical conditions (E–NE winds), what is observed is a reversal of the shelf

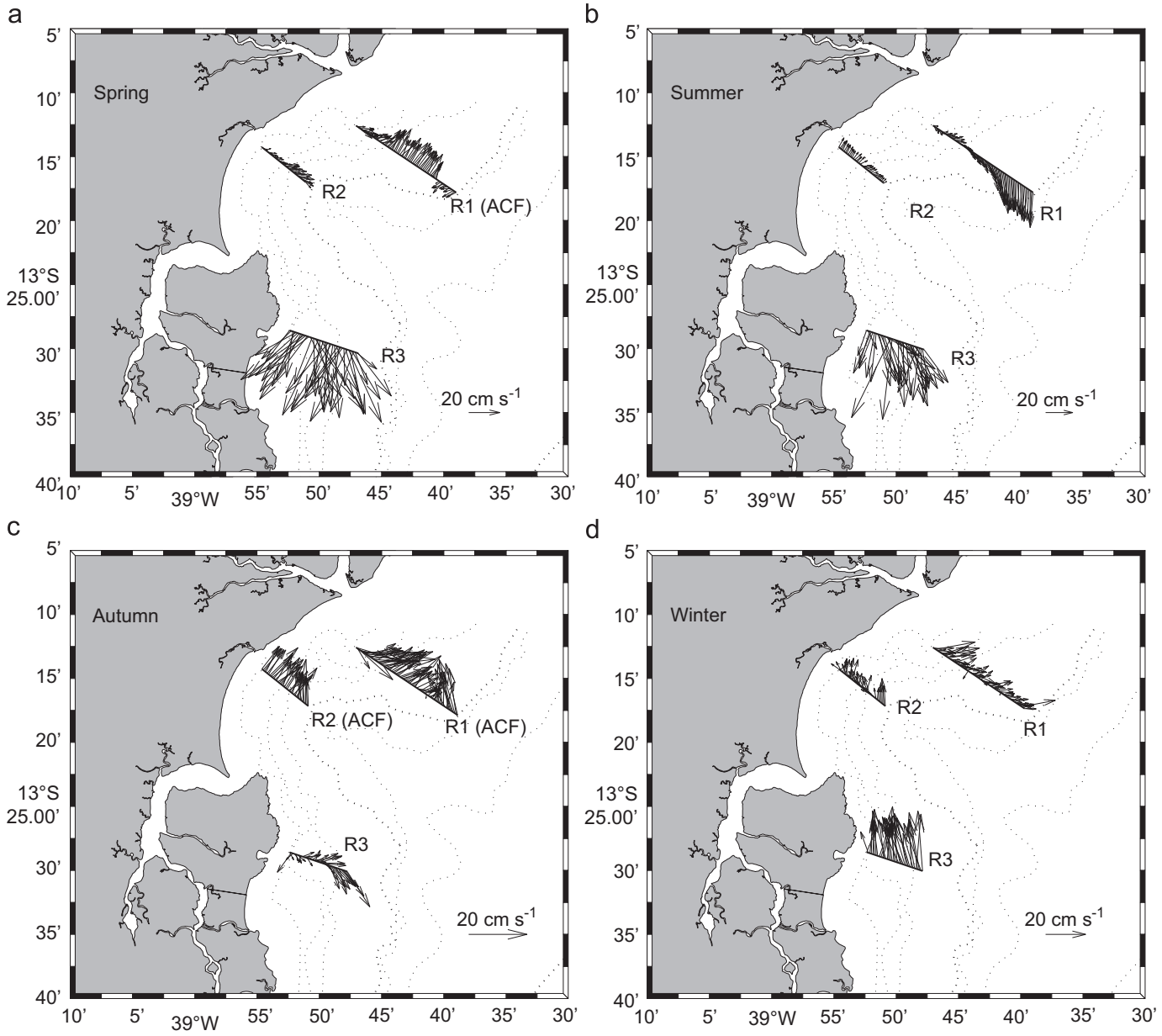

Fig. 6. ADCP derived depth-averaged currents during the (a) spring, (b) summer, (c) autumn and (d) winter cruises, at transects R1, R2 and R3. The isobaths are represented by the 10 m, 20 m, 30 m, 50 m, 200 m, 1000 m and 2000 m contours. The 50 m isobath is in bold. The acronym ACF was used to indicate the transects where the data were obtained after the passage of a Cold Front.

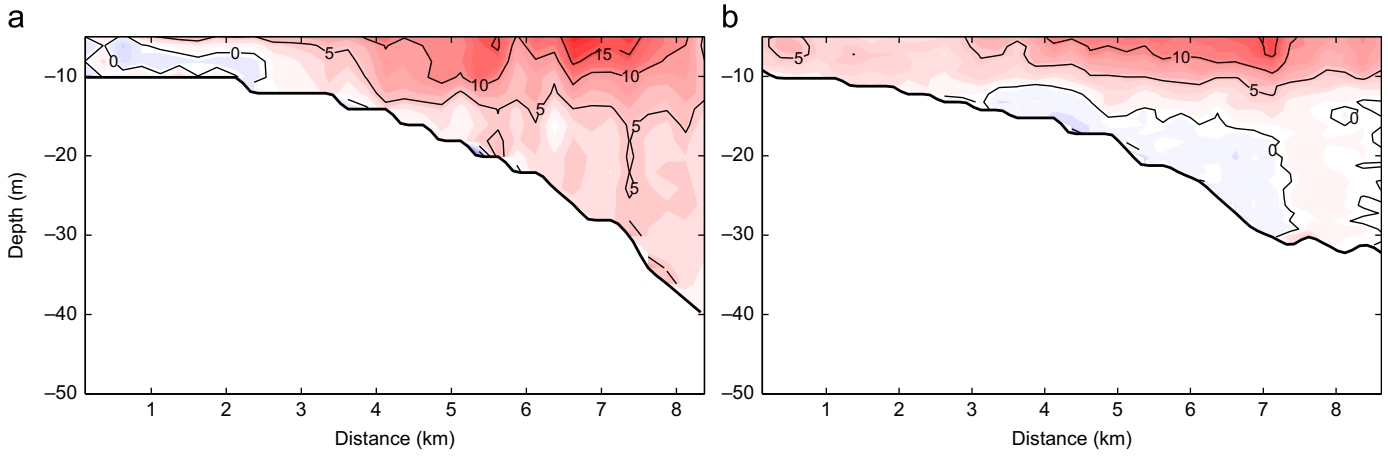

Fig. 7. ADCP derived cross-shore component of the velocity (cm s^{-1}) at transect R2, during the (a) spring and (b) summer cruises. Positive values (in red) are offshore. Distances are from the near coastal station (see Fig. 2 for location). (For interpretation of the references to color in this figure legend, the reader is referred to the web version of this article.)

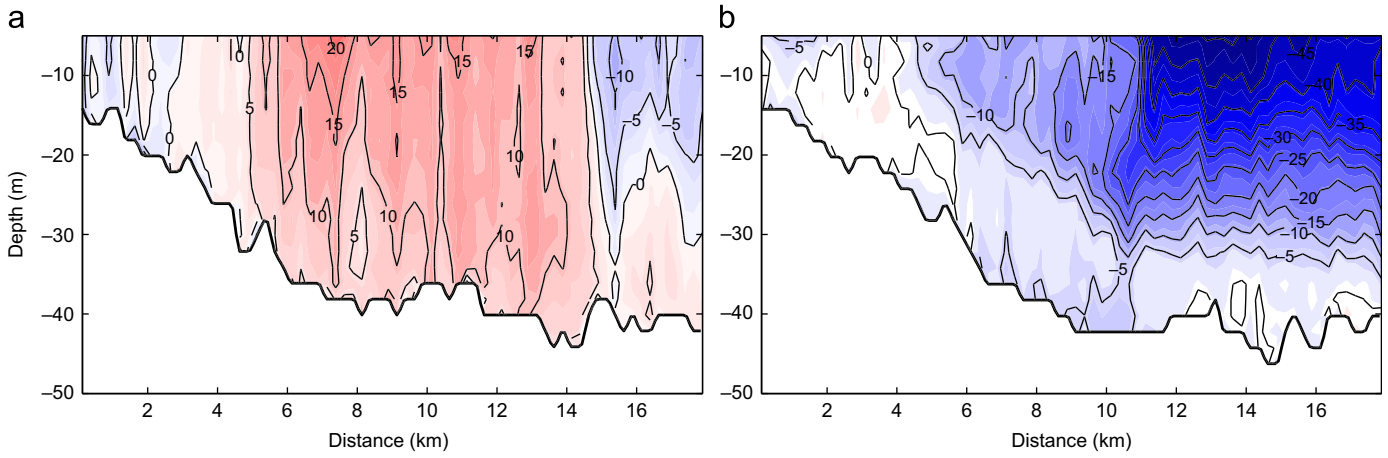

Fig. 8. ADCP derived alongshore component of the velocity (cm s^{-1}) at transect R1, during the (a) spring and (b) summer cruises. Positive values (in red) are to the northeast. Distances are from the near coastal station (see Fig. 2 for location). (For interpretation of the references to color in this figure legend, the reader is referred to the web version of this article.)

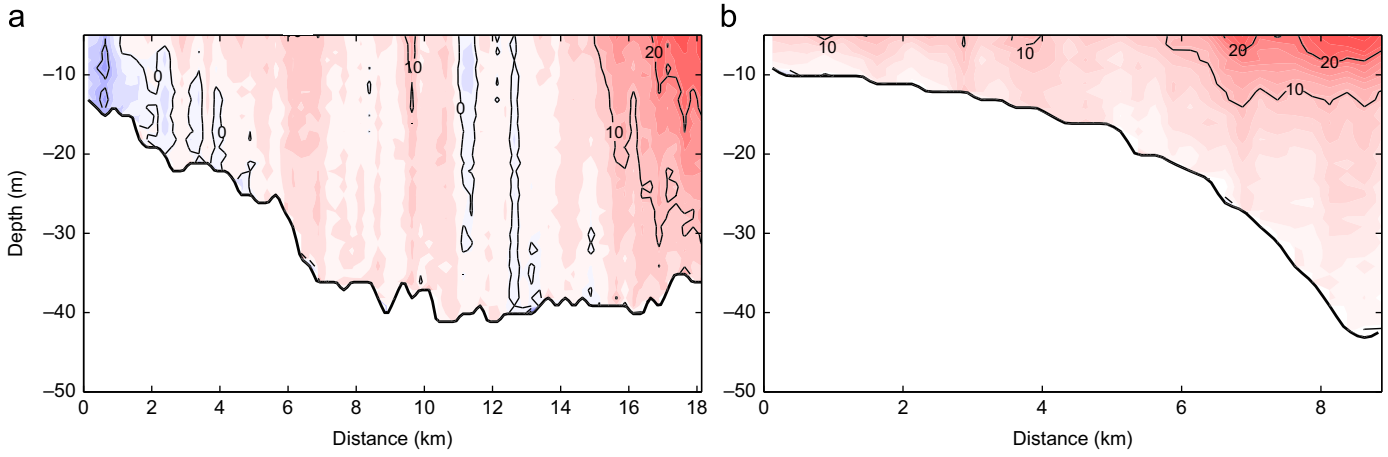

Fig. 9. ADCP derived alongshore component of the velocity (cm s^{-1}) at (a) transect R1 and (b) R2 during the autumn cruise. Positive values (in red) are to the northeast. Distances are from the near coastal station (see Fig. 2 for location). (For interpretation of the references to color in this figure legend, the reader is referred to the web version of this article.)

circulation, with the flow being northeast oriented, the alongshore component being reduced and the cross-shore component being magnified (Fig. 6a and b), which can be seen in more detail in Fig. 7.

As mentioned in Section 2, it is important to remember that transect R2 is located adjacent to the head of Salvador Canyon, a narrow canyon that has a shallow rim. The dynamics observed here is somehow compatible to what is observed in the literature

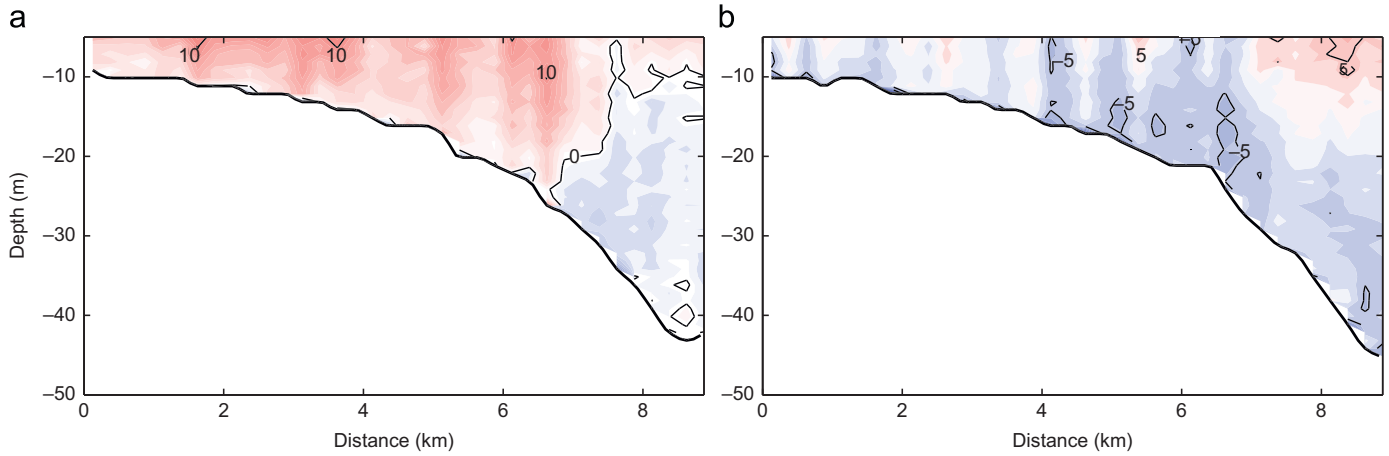

Fig. 10. ADCP derived cross-shore component of the velocity (cm s^{-1}) at transect R2, during the (a) autumn and (b) winter cruises. Positive values (in red) are offshore. Distances are from the near coastal station (see Fig. 2 for location). (For interpretation of the references to color in this figure legend, the reader is referred to the web version of this article.)

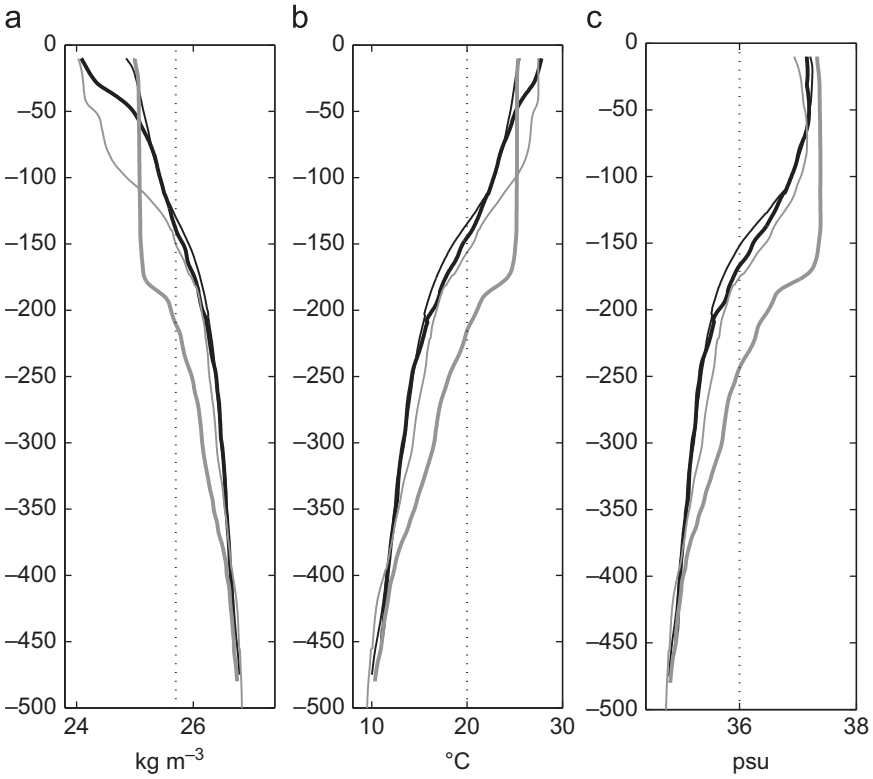

Fig. 11. Mean (a) σ_θ, (b) temperature and (c) salinity vertical profiles of the outer-shelf and slope region (depths >100 m, see Fig. 2 for location) during the spring (light black line), summer (heavy black line), autumn (light gray line) and winter (heavy gray line) seasons. Dotted lines represent the limits between the Tropical Water and the South Atlantic Central Water.

(Hickey, 1997; She and Klinck, 2000). For an upwelling favorable current, a cyclonic circulation at the canyon mouth is generated, cross-shore exchanges are magnified and upwelling at the canyon, when compared to the surrounding shelf-break regions, is enhanced. These results will be described in detail in Section 4.3. Considering that the canyon rim is at a depth of 50 m, which is similar to the vertical stratification scale (minimum value of 40 m during summer), the canyon is expected to influence the circulation along the whole water column. The vertical structure of the cross-shore flow that connects the shelf region with the head of the canyon is presented in Fig. 7 and shows the offshore flow at the upper layers that is associated to the upwelling process that occurs at the shelf/slope region.

At transect R1, which is affected by the downstream flank of the canyon, an additional signature of the cyclonic circulation can be observed in the summer cruise (Fig. 6b). Despite the measurements were taken under typical summertime conditions (E–NE upwelling favorable winds), the flow at the inner portion of the transect is to NE, following the flow direction observed at transect R2, while a 50 cm s^{-1} surface southward oriented flow occupies a great portion of the shelf with a significant vertical shear (Fig. 8b). During the spring cruise, the passage of a strong Cold Front before

the realization of transect R1 (Fig. 4a) did not allow one to verify a similar pattern, since it contributed to a total reversal of the shelf current (Fig. 6a). However, a feature to be explored is that at the end of the ADCP transect a mean SW flow was maintained, with surface velocities of about 15 cm s^{-1} and some vertical shear (Fig. 8a). This flow appears to be related to the circulation at the shelf/slope region. In both spring and summer cruises, the AVISO surface geostrophic currents show a southward oriented WBC at the study region (Fig. 5a and b).

During autumn and winter seasons, the prevailing winds are now from the S/SE and currents are downwelling favorable. With the exception of transect R3 during autumn cruise, a complete reversal of the mean flow was observed, with northeastward oriented currents at all transects (Fig. 6c and d). When relating to the spring/summer scenario, few differences now occur. During the passage of Cold Front systems, the shelf circulation is magnified (transects R1 and R2 in Fig. 6c compared to Fig. 6d), the influence of the WBC (Fig. 5c) becomes more clear during these events and the vertical shear in the velocity field is reduced (Fig. 9a). The reduction of the vertical shear is probably associated to the fact that the WBC is now downwelling favorable and the MLD is deeper.

At transect R2, the influence of the canyon, when compared to the spring/summer scenario is reduced and the alongshore component of the velocity is enlarged (Fig. 9b compared to Fig. 10a). The reduction of the cross-shore flow when a canyon is affected by a downwelling favorable current (Fig. 10a and b) when compared to the case of an upwelling favorable current (Fig. 7a and b) is in agreement with the results of She and Klinck (2000). Despite the reduction of the strength, the general pattern of the cross-shore circulation reverses from the spring/summer scenario to the autumn/winter scenario.

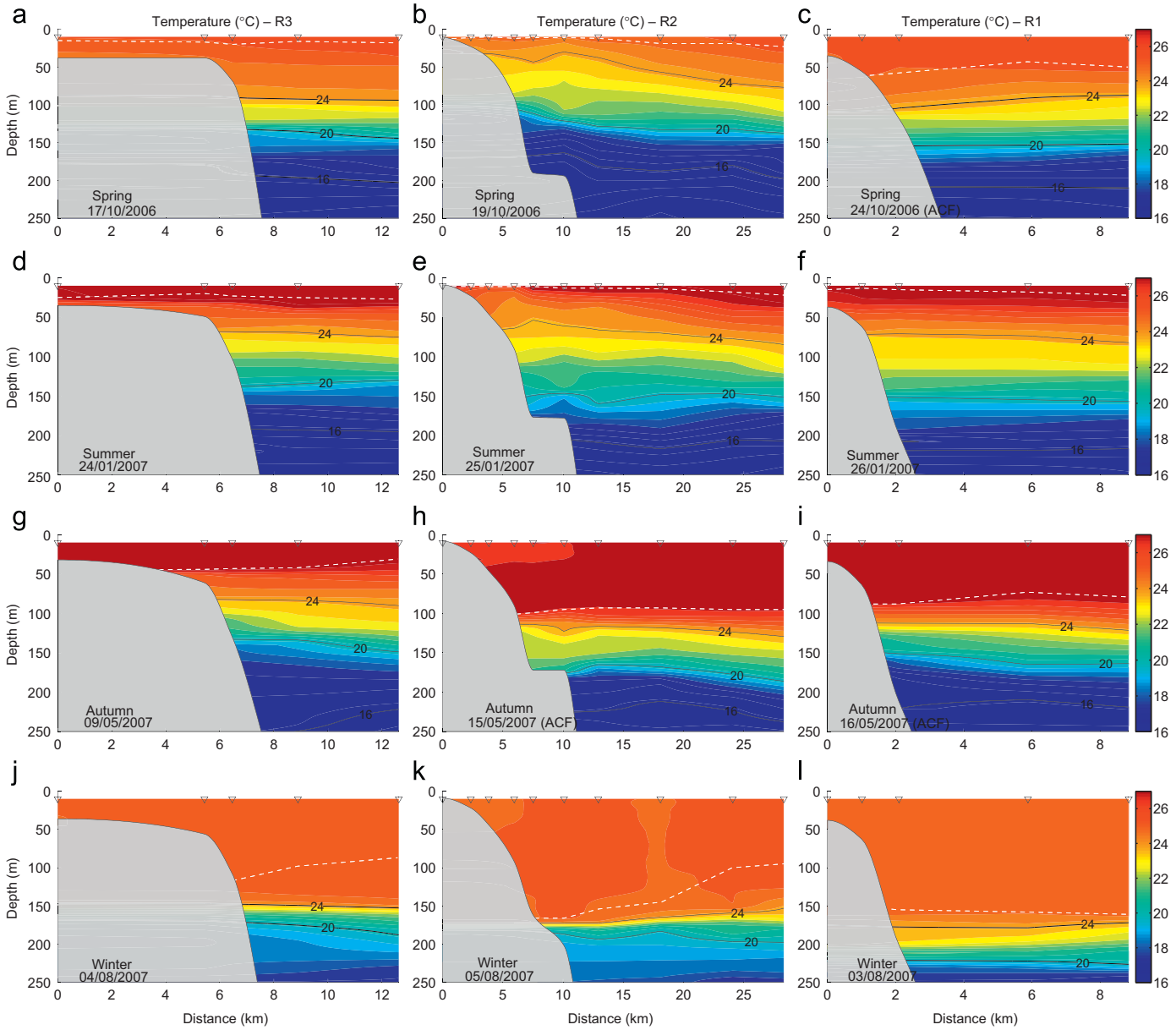

Fig. 12. Temperature vertical sections during the (a–c) spring, (d–f) summer, (g–i) autumn and (j–l) winter cruises at transects R1, R2 and R3. With the exception of the winter cruise, the plots are in chronological order, from left to right, and from top to bottom. The white dashed lines represent the mixed layer depth. Distances between CTD stations (∇) are from the fifth station for transects 1 and 3, and from the second station for transect 2 (see Fig. 2 for location). The acronym ACF was used to indicate the transects where the data were obtained after the passage of a Cold Front.

4.3. Hydrography

In order to provide an overview of the seasonal variation of the hydrographic data sampled at the three transects during each cruise, vertical mean profiles of temperature, salinity and sigma-θ for the outer-shelf (depths >100 m) stations were performed and are presented in Fig. 11. The hydrography of the shelf and shelf/slope region is then discussed in more detail in the sequence of this section.

Fig. 11 shows the presence of two water masses, the warm and salty Tropical Water (TW) and the South Atlantic Central Water (SACW). The TW changed seasonally, being warmer and with almost constant salinity during summer. During spring and winter seasons, the temperature of the upper waters was lower and salinity was more variable. The SACW, which occupied mainly the thermocline, showed almost no change in the thermohaline structure, with the exception of winter, when a deepening of the interface between these two water masses was observed.

The progressively deepening of the isothermal layer (temperature variation $\leq 0.2^{\circ}$C) from 20 m (summer) to ~ 170 m (winter) is presented in Fig. 11b. Changes in the thickness of the isothermal layer can be attributed to the mixing, enhanced by the local winds and to the stratification rupture due to the top water cooling. As will be pointed out later, in the study region, local and large scale dynamics, also contributed to changes in the isothermal layer. The mean temperature at the isothermal layer varied from a maximum of 27.8°C during summer to a minimum of 25°C during winter. Due to the deepening of the isothermal layer during the winter season, warm waters occupied the depths below 100 m in comparison to the other seasons (Fig. 11b, heavy gray line). The thermocline region was mainly occupied by the SACW, starting at depths of ~ 150 m (~ 220 m) during the summer (winter) season. Changes in the upper salinity were less pronounced, with the maximum value of 37.3 being registered during wintertime, when the salinity values along depth were higher than the other seasons (Fig. 11c).

With the purpose of evaluating the influence of winds, local topography and transient processes on the seasonal changes of the hydrographic properties, the vertical distribution of temperature for the shelf/slope region is presented in Fig. 12 for all cruises and the results are compared with the climatological MLD values obtained from Montégut et al. (2004) (Fig. 3).

During the spring season, the hydrographic measurements made at transects R2 and R3 were under typical conditions, with E–NE mean winds of 2.7 m s^{-1} (Fig. 4a). The observed MLD at transects R2 and R3 was less than 12 m (Fig. 12a and b), which does not agree neither with the climatological value (~ 35 m, Fig. 3a) nor with the surface Ekman layer depth (D_E) of about 46 m, according to the Stewart (2005) formulation ($D_E = 7.6U_{10}/\sqrt{\sin|\varphi|}$), where U_{10} is the wind speed at 10 m above the sea and φ is the latitude of reference.

Considering that transect R2 is located at the Salvador Canyon head (Fig. 2) and in accordance with what was observed by She and Klinck (2000), upwelling from depths of up to 200 m is

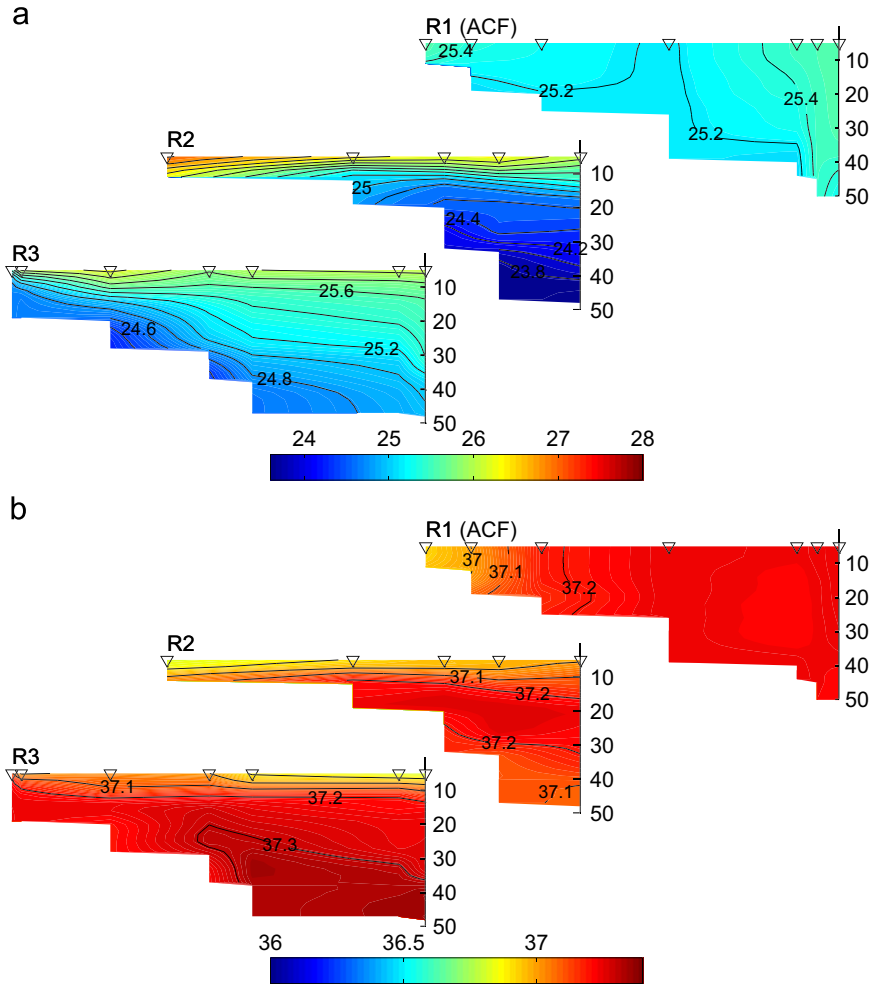

Fig. 13. Cross-shelf (depths <100 m) sections of (a) temperature and (b) salinity for transects R1, R2 and R3 during the spring cruise. The hydrographic stations are represented by ∇ (see Fig. 2 for location). The acronym ACF was used to indicate the transects where the data were obtained after the passage of a Cold Front.

observed in the region (Fig. 12b). Since the canyon rim is very shallow and the vertical stratification scale is of the same order, the whole water column above the rim is also affected by the canyon dynamics. In analogy to what was observed by Hickey (1997), the upwelling at the depth of the rim results in a compression of the layers (see Fig. 13a for a detailed view at the upper layer), while at greater depth layers are stretched. The trapped cyclonic circulation resulted from the interaction of this upwelling favorable current with the canyon topography, as described by Hickey (1997) and She and Klinck (2000), is also clearly seen at this transect, where the center of the cell is approximately located at 10 km in Fig. 12b.

While the upwelling at transect R2 is mostly enhanced by the local canyon topography, at the adjacent shelf (transect R3, Fig. 12a), the shortening of the MLD when compared to the climatology seems to be influenced by the circulation at the shelf/slope region, where the interaction of the two anti-cyclonic cells that occurs at the surroundings of the study area (Fig. 5a) generates a relatively low pressure system which can contribute to raise the MLD near the coastal region. Campos et al. (2000), at the Southeast Brazilian Bight, where the shelf is wider than the EBS, argue that the combined effect of coastal wind-driven upwelling and meander induced upwelling during the summer, results in a strong mechanism capable of bringing cold waters from the slope regions to near the coast. According to the authors, during wintertime, when coastal upwelling is diminished, practically only the meander-induced upwelling occurs.

The measurements taken at R1 transect, still during the spring season, but under the influence of a strong Cold Front (mean SE wind of 5.7 m s^{-1}, Fig. 4a) shows that the MLD drooped to about 50 m depth (Fig. 12c), a value lower than the depth of the surface Ekman layer (DE $\cong$ 90 m) due to the mean downwelling favorable wind. At Fig. 12c, a strongly homogeneous scenario could also be observed at the R1 shelf with almost no change over the shelf neither in temperature (Fig. 13a) nor salinity (Fig. 13b).

The cruise made during the summer season did not experience the passage of a Cold Front, being made under typical summertime conditions (upwelling favorable NE winds, Fig. 4b). Once again, the MLD did not agree neither with the climatological mean for this season ($\sim$35 m, Fig. 3b) nor with the Ekman layer depth (DE $\cong$ 58 m), reaching depths of less than 15 m at transect R3 and being almost non-existent at transects R1 and R2 (Fig. 12d–f). Here, in analogy to what was observed in transect R2 during springtime, the canyon topography enhances upwelling (Fig. 12b and e), when compared to the surrounding shelf regions located at transects R1 and R3, and a cyclonic trapped circulation at the canyon is again observed. This cyclonic circulation also affects the coastal region north of the canyon head, leading to a downward of the isotherms at the inner shelf (Fig. 14a, R1) and a weak northeastward flow (Fig. 6b, R1). At the canyon head, in transect R2, this downward of the isotherms occurs at the shelf and shelf-break region and lays underneath of an intense stratification in the top 20 m of the water column. At transect R3 (Fig. 12d), in analogy with what observed at transects R1 and R2

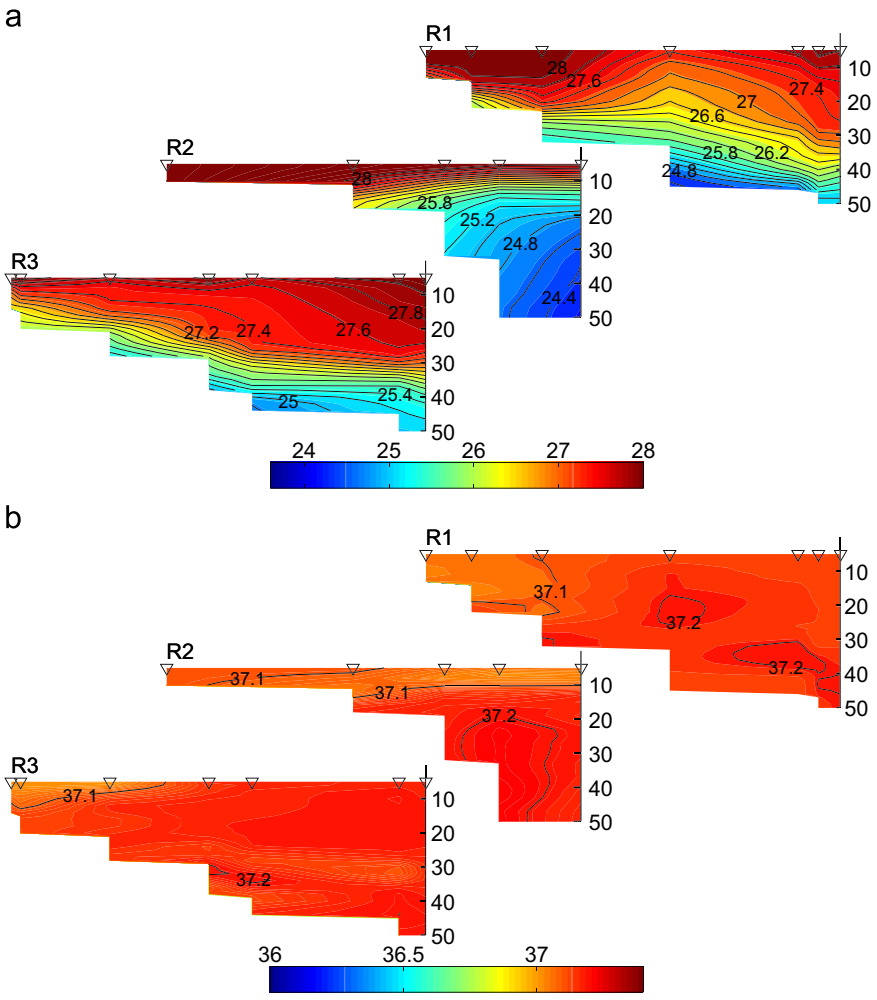

Fig. 14. Cross-shelf (depths $<$100 m) sections of (a) temperature and (b) salinity for transects R1, R2 and R3 during the summer cruise. The hydrographic stations are represented by ∇ (see Fig. 2 for location).

(Fig. 12e and f), a strongly stratified scenario is observed in the upper layers, and the relatively cold water intrusion that occurs in the shelf is a result of the prevailing upwelling favorable winds alone (Fig. 14a, R3). Overall, the summertime salinity at transects R1–R3 showed a strong homogeneity (Fig. 14b).

During the autumn cruise, a strong Cold Front was observed in the middle of the cruise (Fig. 4c), affecting the R1 and R2 transects. The MLD at transect R3 (under typical autumn conditions) reached 45 m depth (Fig. 12g) and is in agreement with the climatological value presented in Fig. 3c and with the Ekman layer depth of about 42 m. Although at transect R3 the shelf region temperature was very homogeneous, a moderate vertical stratification was presented in the salinity field (Fig. 15a and b).

After the passage of the Cold Front, a drop in the temperature was observed at the shelf region of transects R1 and R2, although water was still kept homogeneous. Salinity horizontal gradients started to develop, with less saline waters along the inner-shelf (Fig. 15, R1 and R2), which supports the northeastward shelf currents (Fig. 6c, R1 and R2). Cirano and Lessa (2007), studying the oceanography of Todos os Santos Bay, located about 42 km from the northwest border of the study region, found May to be the month with the largest net inflow of freshwater (only evaporation–precipitation flux) and one of the largest climatological monthly values of overall freshwater inflow (evaporation–precipitation flux and fluvial discharges). During the wet period, but for July, these authors also found mean salinity values of 35.8 (surface) and 36.8 (bottom) at the adjacent shelf (at a water column of 33 m). These less haline values found at the shelf region during the autumn cruise are consistent with the results of Cirano and Lessa (2007) and reflect the influence (although small) of the continental drainage. The major rivers surrounding the study region are located at the Todos os Santos Bay. At Camamu Bay, located about 60 km to the south, river discharges are lower and do not change significantly between seasons (Amorim et al., 2011).

At the shelf/slope region of transects R1 and R2, the MLD drooped to about 100 m depth (Fig. 12h and i), which is almost twice of the climatological value (Fig. 3c) but strongly agrees with the Ekman layer depth of 105 m due to the mean downwelling favorable winds of 6.6 m s^{-1} (Fig. 4c), although the MLD also depends on the past history of the local wind, and the Ekman depth is expected to be rather less than the MLD if the latter was influenced by short periods of strong winds (Pond and Pickard, 1983), which was the case prior to the realization of transects R1 and R2. Not only that, as shown in Fig. 5c, the region of study is largely influenced by a WBC, which is downwelling favorable. In addition, at least for transect R2 (Fig. 12h), the vertical mixing may have been enhanced by the intensification of the downwelling system due to the canyon, as reported by She and Klinck (2000). The effects of the canyon topography also contributed to form an anti-cyclonic circulation at the thermocline region of transect R2 ($\sim$150 m depth).

Finally, the winter cruise was made under typical wintertime conditions (S–SE winds, Fig. 4d) and did not experience the

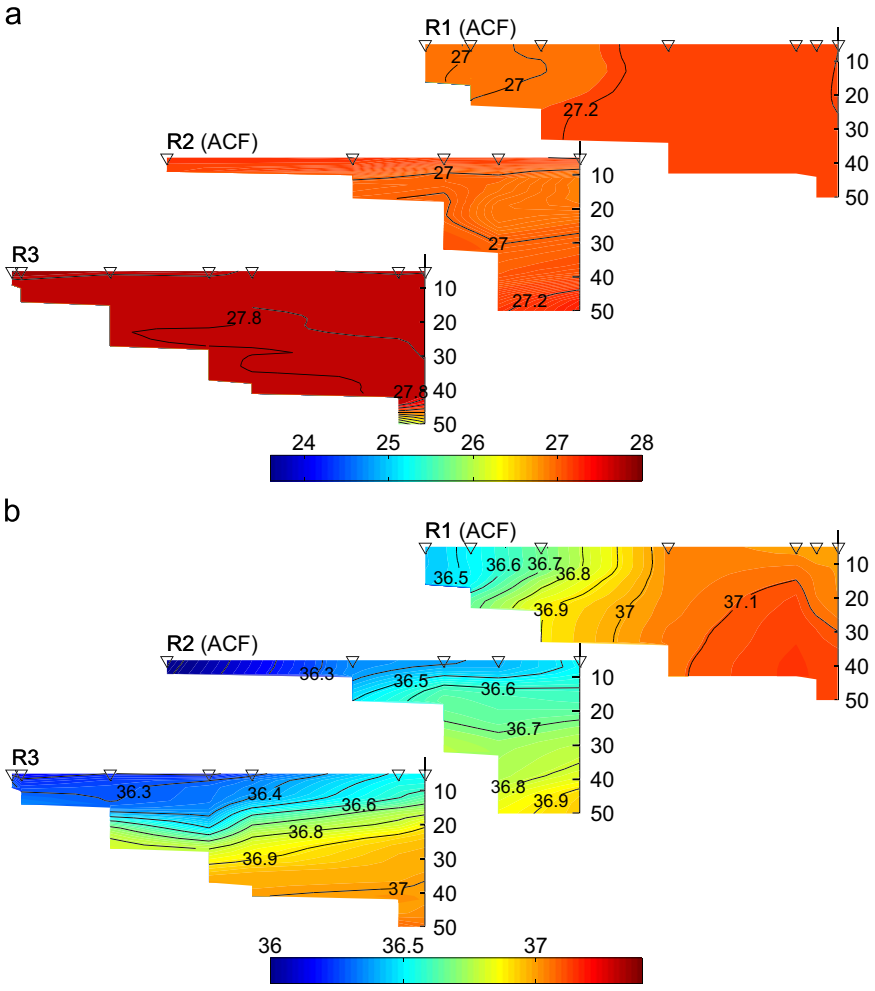

Fig. 15. Cross-shelf (depths <100 m) sections of (a) temperature and (b) salinity for transects R1, R2 and R3 during the autumn cruise. The hydrographic stations are represented by ∇ (see Fig. 2 for location). The acronym ACF was used to indicate the transects where the data were obtained after the passage of a Cold Front.

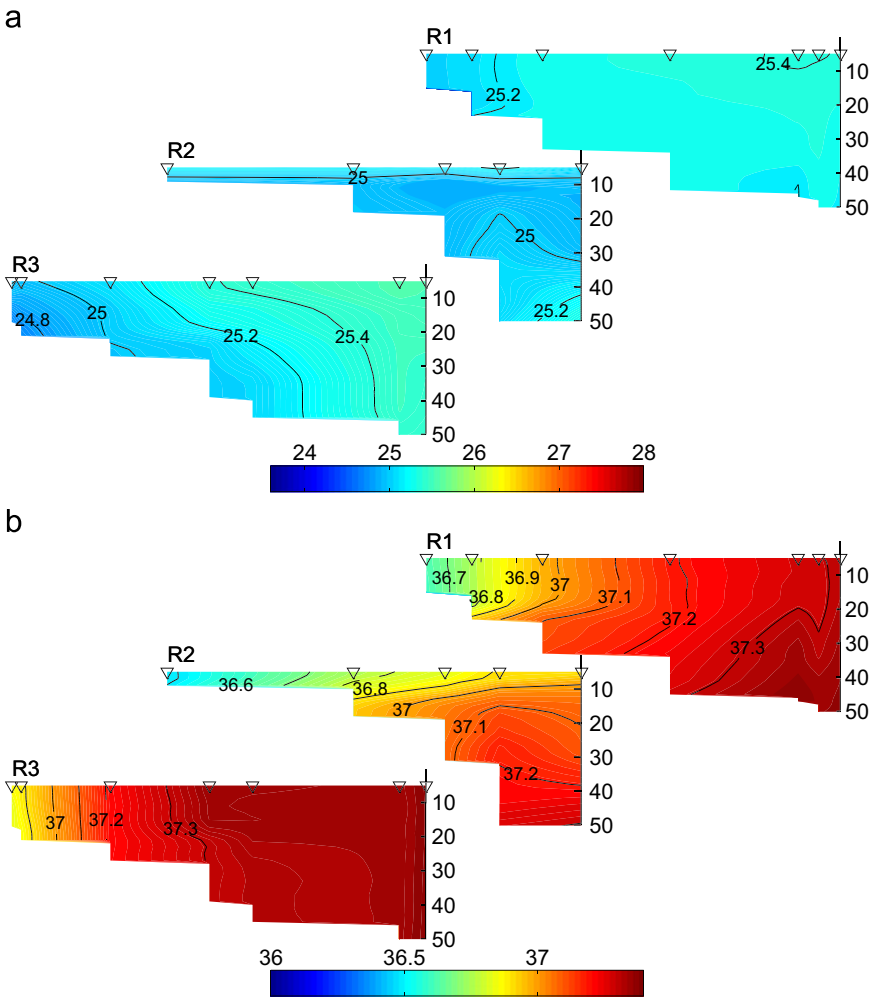

Fig. 16. Cross-shelf (depths < 100 m) sections of (a) temperature and (b) salinity for transects R1, R2 and R3 during the winter cruise. The hydrographic stations are represented by ∇ (see Fig. 2 for location).

passage of a Cold Front system. Here, a deeper MLD (depth > 120 m) was observed at all transects (Fig. 12j–l), with values significantly higher than the climatological value of 75 m (Fig. 3d). At transect R2, in analogy to what was observed during the autumn cruise, the presence of the canyon, certainly contributed to the deepening of the MLD. But, probably, the most reasonable explanation for this deepening of the MLD at all transects is the interaction with the shelf–slope current, which is downwelling favorable. If one considers that the bifurcation of the SEC reaches its most southern position (17°S) in July, this period is probably affected by more episodes of intense northward WBC, such as the one that occurred at the beginning of August (Fig. 5d). At the shelf region, although temperature is very homogeneous (Fig. 16a), the continental drainage, in a similar way to what was observed during the autumn cruise, seemed to affect the coastal region, where horizontal (at transects R1 and R3) and vertical (at transect R2) gradients of salinity (Fig. 16b) are observed.

5. Summary and conclusions

The physical properties observed at the Eastern Brazilian Shelf (centered at 13°S) and associated slope region during the four original seasonal cruises were able to show the variety of forcing mechanisms that the region is exposed, which include, the local winds and topography, transient processes and interaction with meso/large scale circulation. The major features to be pointed out are: (i) the outer-shelf was influenced by the meso/large scale dynamics and local topography; (ii) inner and mid-shelves were influenced by the local winds and by the dynamics associated with the local topography; and (iii) the whole system was influenced by the seasonal changes in the large scale and atmospheric circulation and transient events, presenting very distinct scenarios between spring/summer and autumn/winter seasons.

During the austral spring and summer seasons, the prevailing upwelling favorable winds blowing from E–NE were responsible for driving southwestward shelf currents. The interaction with the Western Boundary Current (the Brazil Current), especially during summer, was significant and a considerable vertical shear in the velocity field was observed at the outer shelf. The passage of a Cold Front system during the springtime caused a complete reversal of the mean flow and contributed to the deepening of the Mixed Layer Depth (MLD) at transect R1. In addition, the presence of a steep topography at transect R2, the Salvador Canyon, added more features to the local circulation during these seasons.

A scale analysis has shown that Salvador Canyon is a narrow canyon, implying that the alongshore geostrophic balance within the canyon could not be maintained ($S \gg 1$). According to Hickey (1997) and She and Klinck (2000), an upwelling favorable current passing through a canyon, would drive relatively cold fluid upward and into the canyon, causing an abrupt shift of the isotherms and enhancing the upwelling system, when compared to the upwelling observed at the adjacent shelf. A cyclonic trapped circulation would also be formed at the rim depth and below. At transect

R2, and considering that the depth of the canyon's rim is comparable to the vertical stratification scale, the whole water column above the canyon rim seems also to be affected by the presence of the canyon. During both spring and summer cruises, upwelling is largely intensified at the canyon, the adjacent shelf currents at the head of the canyon had the cross-shore component of the velocity enlarged and a cyclonic trapped circulation was observed at the canyon. During summertime, this circulation also seemed to affect the adjacent coastal downward region at transect R1.

The MLD during the spring and summer seasons was influenced by the local canyon topography, transient processes and interaction with the large-scale circulation. The climatological MLD for these seasons is about 30 m depth, but depths less than 15 m were observed at all transects under typical conditions. This behavior could be attributed to the combined effect of the coastal wind-driven upwelling and meander induced upwelling, which at transect R2 were magnified by the upwelling enhanced by the canyon.

During the austral autumn and winter seasons the prevailing downwelling favorable winds blowing from the SE acted to total reverse the shelf circulation, resulting in a northeastward flow. The passage of a strong Cold Front, during the autumn season, contributed not only to the strengthening of the flow but also to the deepening of the MLD at transects R1 and R2, due to the intensification of the vertical mixing. According to Hickey (1997) and She and Klinck (2000), a downwelling favorable current passing through a canyon would lead to a somehow opposite dynamics, when compared to the upwelling situation, with the exception that cross-shore exchanges are reduced. During both autumn and winter cruises, an intensification of the downwelling process was observed at the canyon and the alongshore velocity at the shelf region adjacent to the head of the canyon was less affected when compared to the upwelling situation. During the autumn cruise, an evidence of an anticyclonic circulation at 150 m depth was also found.

In addition, the MLD observed during the winter season at all transects appeared to be strongly influenced by the shelf–slope circulation and the episodes where the Western Boundary Current is northward and downwelling favorable. During this seasonal cruise, no Cold Front system was observed, but the MLD reached a deeper depth (>150 m) when compared to the climatological mean value of about 70 m.

Acknowledgments

This research was supported by PETROBRAS and approved by the Brazilian oil regulatory agency ANP (Agência Nacional de Petróleo, Gás Natural e Biocombustíveis), within the special participation research project Oceanographic Modeling and Observation Network (REMO). Fabiola N. Amorim was supported by Brazilian scholarships from CAPES and REMO. Mauro Cirano and Edmo J.D. Campos were supported by CNPq Research grants. We thank PETROBRAS for releasing the data sets obtained under the project "Programa de Levantamento de dados oceanográficos do BCAM-40 (Contrato 4600216176)" and MSc Saulo Spano, the field coordinator during the BCAM-40 seasonal cruises, who made the cruises far more easier and enjoyable for the whole scientific crew. We also thank the two anonymous referees for their thoughtful comments.

References

Allen, J.S., Beardsley, R.C., Blanton, J.O., Biocourt, W.C., Butman, B., Coachman, L.K., Huyer, A., Kinder, T.H., Royer, T.C., Shumacher, J.D., Smith, R.L., Strurges, W., 1983. Physical oceanography of continental shelves. Reviews of Geophysics and Space Physics 21 (5), 1149–1181.

Allen, S.E., Durrieu de Madron, X., 2009. A review of the role of submarine canyons in deep-ocean exchange with the shelf. Ocean Science 5, 607–620.

Amorim, F.N., Cirano, M., Soares, I.D., Lentini, C.A.D., 2011. Coastal and shelf circulation in the vicinity of Camamu Bay (14°S), Eastern Brazilian Shelf. Continental Shelf Research 31, 108–119.

AVISO, 2011. SSALTO/DUACS User Handbook: (M)SLA and (M)ADT Near-Real Time and Delayed Time Products. Technical Report, 49 pp. Centre National D'études Spatiales, CLS-DOS-NT-06-034-Issue 2.4.

Campos, E.J.D., Velhote, D., Silveira, I.C.A., 2000. Shelf break upwelling driven by Brazil Current cyclonic meanders. Geophysical Research Letters 27 (6), 751–754.

Cirano, M., Lessa, G.C., 2007. Oceanographic characteristics of Baía de Todos os Santos, Brazil. The Revista Brasileira de Geofísica 25 (4), 363–387.

Cirano, M., Mata, M.M., Campos, E.J.D., Deiró, N., 2006. A circulação oceânica de larga-escala na região oeste do Atlântico Sul: validação da climatologia anual com base no modelo de circulação global OCCAM. The Revista Brasileira de Geofísica 24, 209–230.

Dominguez, J.M.L., 2006. The coastal zone of Brazil—an overview. The Journal of Coastal Research 39 (Special Issue), 16–20.

Emery, W.J., Thomson, R.E., 1997. Data Analysis Methods in Physical Oceanography. Pergamon Press, New York, 400 pp.

Gonzalez-Pola, C.J., Fernández-Días, J.M., Lávin, A., 2007. Vertical structure of the upper ocean from profiles fitted to physically consistent functional forms. Deep-Sea Research 54, 1985–2004.

Hickey, B.M., 1997. The response of a steep-sided narrow canyon to time-variable wind forcing. Journal of Physical Oceanography 27 (5), 697–726.

Hsu, S.A., 1986. Correction of land-based wind data for offshore applications: a further evaluation. Journal of Physical Oceanography 16, 390–394.

INPE, C., 2009a. Climanálise—boletim de monitoramento e análise climática, vols. 21 and 22. 〈http://www6.cptec.inpe.br/revclima/boletim/〉.

INPE, C., 2009b. Plataforma de coleta de dados meteorológicos. 〈http://satelite.cptec.inpe.br/PCD/historico/〉.

Kampf, J., 2006. Transient wind-driven upwelling in a submarine canyon: a process-oriented modeling study. Journal of Geophysical Research 111, C11011. doi:10.1029/2006JC003497.

Kanamitsu, M., Ebisuzaki, W., Woollen, J., Yang, S.K., Hnilo, J.J., Fiorino, M., Potter, G.L., 2002. NCEP-DOE AMIP-II reanalysis (R-2). The Bulletin of the American Meteorological Society 83 (11), 1631–1643.

Knoppers, B., Ekau, W., Figueiredo, A.G., 1999. The coast and shelf of east and northeast Brazil and material transport. Geo-Marine Letters 19 (3), 171–178. doi:10.1007/s003670050106.

Lee, T.N., Ho, W.J., Kourafalou, V., Wang, J.D., 1984. Circulation on the continental shelf of the Southeastern United States. Part I: subtidal response to wind and Gulf stream forcing during winter. Journal of Physical Oceanography 14, 1001–1012.

Liu, P.C., Schwab, D.J., Bennett, J.R., 1984. Comparison of a two-dimensional wave prediction model with synoptic measurements in Lake Michigan. Journal of Physical Oceanography 14, 1514–1518.

Montégut, C.D., Madec, G., Fischer, A.S., Lazar, A., Iudicone, D., 2004. Mixed layer depth over the global ocean: an examination of profile data and a profile-based climatology. Journal of Geophysical Research 109, C12003. doi:10.1029/2004JC002378.

Oliveira, L.R., Piola, A.R., Mata, M.M., Soares, I.D., 2009. Brazil current surface circulation and energetics observed from drifting buoys. Journal of Geophysical Research 114, C10006. doi:10.1029/2008JC004900.

Pereira, A., Belem, A., Castro, B.M., Geremias, R., 2005. Tide–topography interaction along the Eastern Brazilian Shelf. Continental Shelf Research 25, 1521–1539.

Pond, S., Pickard, G.L., 1983. Introductory Dynamical Oceanography. Pergamon Press, Oxford, 329 pp.

Rezende, L.F., Silva, P.A., Cirano, M., Peliz, A., Dubert, J., 2011. Mean circulation, seasonal cycle and eddy interactions in the Eastern Brazilian Margin, a Nested ROMS model. Journal of Coastal Research 27 (2), 329–347.

Rodrigues, R.R., Rothstein, L.M., Wimbush, M., 2007. Seasonal variability of the South Equatorial Current bifurcation in the Atlantic Ocean: a numerical study. Journal of Physical Oceanography 37 (1), 16–30.

She, J., Klinck, J.M., 2000. Flow near submarine canyon driven by constant winds. Journal of Geophysical Research 105 (C12), 28671–28694.

Silveira, I.C.A., Miranda, L.B., Brown, W.S., 1994. On the origins of the North Brazil current. Journal of Geophysical Research 99 (C11), 22501–22512.

Silveira, I.C.A., Schmidt, A.C.K., Campos, E.J.D., Godoi, S.S., Ikeda, Y., 2000. A Corrente do Brasil ao largo da costa leste Brasileira. Revista Brasileira de Oceanografia 48 (2), 171–183.

Soutelino, R.G., Silveira, I.C.A., Gangopadhyay, A.A.M.J., 2011. Is the Brazil Current eddy-dominated to the north of 20°S? Geophysical Research Letters 38, L03607. doi:10.1029/2010GL046276.

Stewart, H.R., 2005. Introduction to Physical Oceanography. Department of Oceanography, Texas A&M University.

Stramma, L., England, M., 1999. On the water masses and mean circulation of the South Atlantic Ocean. Journal of Geophysical Research 104 (C9), 20863–20883.

Stramma, L., Schott, F., 1999. The mean flow field of the tropical Atlantic Ocean. Deep-Sea Research Part II 46, 279–303.